

A Design Optimization of Asymmetric Air-gap Structure for Small 3-phase Permanent Magnet SPM BLDC Motor

Seung-Han Kam and Tae-Uk Jung*

Department of Electrical Engineering, Kyungnam University, Chang-won 631-701, Korea

(Received 3 February 2015, Received in final form 18 March 2015, Accepted 19 March 2015)

As many researchers are relentlessly trying to improve the power generation schemes from the power grid, to meet the constantly increasing electricity demand. In this paper, the results of a finite element analysis are carried out to study on a design optimization of an asymmetric air-gap structure in 3-phase Permanent Magnet Brushless DC Motors. To achieve a high efficiency for a 3-phase PM BLDC motor, the asymmetric air-gap structure is proposed considering the rotation direction of a motor. Generally, a single-phase BLDC motor is applied asymmetric air-gap structure for starting. This is because the asymmetric air-gap structure causes reluctance variation so the motor can utilize reluctance torque toward a rotation direction. In this paper, the asymmetric air-gap is applied to 3-phase BLDC SPM motor so it utilizes reluctance torque with alignment torque. A proposed model is designed by 2-D FE analysis and the results are verified by experimental test.

Keywords : 3-phase BLDC motor, asymmetric air-gap structure, high efficiency, SPM motor, reluctance torque

1. Introduction

As many researchers are relentlessly trying to improve the power generation schemes from the power grid, to meet the constantly increasing electricity demand; it may be worth to intelligently reducing the load demand. Also, because of the global and local pollution, depletion of fossil fuels, and higher gas prices; ambitious plans for new residential appliances types with less energy consumption have been motivated. PM BLDC motors used in robots or other industrial applications are currently a niche technology in many countries, but they are increasingly expected to form an important role in a low carbon future. This is largely because a future of more efficient pumps is one of the lowest carbon footprint cutting options [1-10]. BLDC motors are being designed in or currently used in power steering, engine cooling fan, fuel/water pump, air conditioning compressor [11-13].

This paper presents an asymmetric air-gap structure of 3-phase PM BLDC motors to improve a higher efficiency. The aim of the proposed structure is to obtain higher output torque by using additional reluctance torque which is produced by an asymmetric air-gap without volume

changes.

Firstly, an existing commercial 3-phase BLDC motor is chosen as an initial model. In order to obtain characteristics of the initial model, finite element analysis (FEA) is processed. Next, based on the results of FEA, the proposed structure is applied and compared with the initial model. Finally, the results of FEA are verified through the experimental results.

2. Structure Design

Generally, SPM type motors have only alignment torque, whereas IPM type motors have total torque which reluctance torque is added to alignment torque. Figure 1 shows

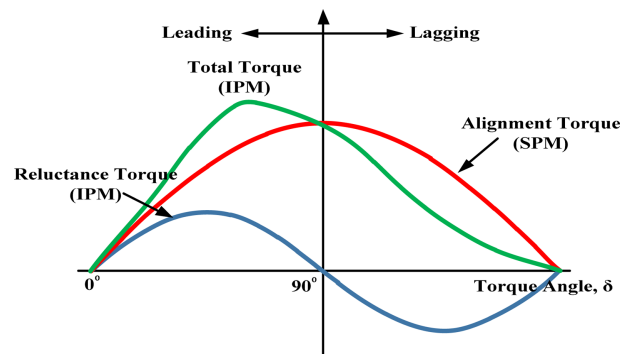


Fig. 1. (Color online) Torque Generation Comparison.

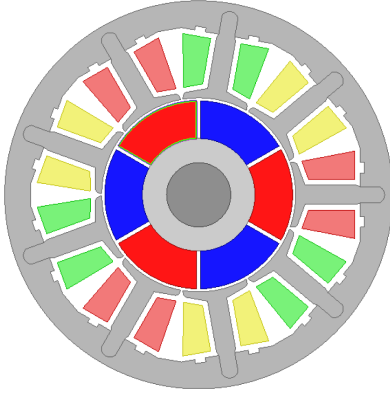


Fig. 2. (Color online) Initial FEM Model.

torque generation of each type. In the case of SPM type, there is a problem with advanced angle control with sensor-less BLDC controller which does not have advanced angle control function. However, the proposed structure application is able to utilize the advanced angle function by asymmetric air-gap.

2.1. Initial Model

A commercial PM BLDC motor is chosen as the initial model as shown in Fig. 2. The initial model is a 3-phase PM BLDC motor and has 6-poles and 9-slots. The permanent magnet of the rotor surface is Bonded-Ferrite magnet. Table 1 shows the specifications of the PM BLDC motor.

2.2. Asymmetric Air-gap Structure

$$T = \frac{1}{2} i^2 \frac{dL}{d\theta} - \frac{1}{2} \phi^2 \frac{dR}{d\theta} + N i \frac{d\phi}{d\theta} \tag{1}$$

Table 1. Specifications of Initial Model.

Parameter	Value
Rated voltage [V]	15
Rated current [A]	0.092
Duty ratio	0.83
Rated output power [W]	1
Rated Speed [rpm]	1580
Number of slots	9
Number of poles	6
Depth of stator [mm]	5
Phase resistance [Ω]	12.9
Number of turns	350
Air-gap length [mm]	0.4
Stator outer diameter [mm]	48
Rotor outer diameter [mm]	24
Core material	S60
Permanent magnet	Bonded Ferrite (Br = 0.284)

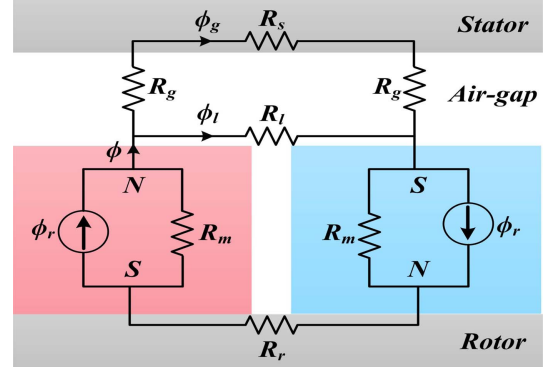


Fig. 3. (Color online) Magnetic Equivalent Circuit Model.

Where, i is current of stator, ϕ is flux from the permanent magnet and N is the number of turns.

The torque term always acts to increase inductance or permeance (since $L = N^2P$) and acts to decrease reluctance. As a result, this term is called reluctance torque. The first two terms are the reluctance torque associated with the coil and magnet respectively, and the third term is the alignment torque due to the mutual flux ϕ linking the magnet to the coil. $dL/d\theta$ is proportional to $-dR/d\theta$, making the first and second terms in (1) equivalent in terms of torque production. In this paper, the reluctance torque is increased by augmenting $dL/d\theta$ or $-dR/d\theta$.

In Figure 3, the rotor and stator steel areas are modeled simply as reluctances R_r and R_s respectively. The two half magnets are modeled as a flux source ϕ_r and associated magnet reluctance R_m , with the direction of the flux source dictating the magnet polarity. Primary flux flow from the magnets across the air gap into the stator flows through the air gap reluctances denoted R_g . Leakage flux from one magnet to the next flows through the leakage reluctance R_l . The three circuit fluxes are the magnet flux ϕ , the air gap flux ϕ_g , and the leakage flux ϕ_l . Rather than solving the magnetic circuit as shown in Fig. 3, it is convenient to simplify the circuit as shown in Fig. 4(a). Since the right magnet and rotor reluctance are in series, they are swapped in Fig. 4(d). This places the two half magnets net to each other and places the rotor reluctance next to description of the leakage reluctance.

Given the magnetic circuit in Fig. 4, the magnet flux ϕ can be expressed using flux division as;

$$\phi = \frac{2R_m}{2R_m + K_r(R_{g_min} + R_{g_max})} \phi_r = \frac{1}{1 + L_r \frac{R_{g_min} + R_{g_max}}{2R_m}} \phi_r \tag{2}$$

Where, R_m is magnet reluctance, K_r is reluctance factor which increases air-gap reluctance slightly to compensate for the missing steel reluctance, and R_{g_min} and R_{g_max} are

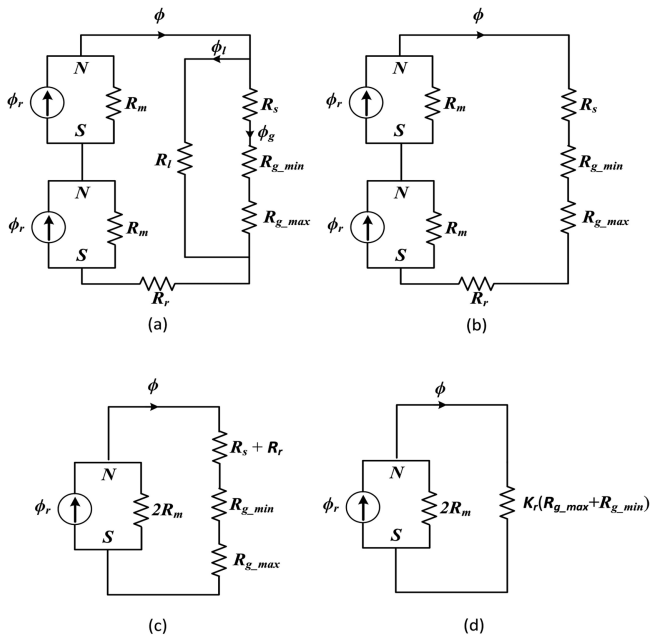


Fig. 4. Simplifications of Magnetic Equivalent Circuit in Fig. 3.

minimum and maximum air-gap reluctance respectively.

The air gap flux can be written as;

$$\phi_g = K_l \phi = \frac{K_l}{1 + K_r \frac{R_{g_min} + R_{g_max}}{2R_m}} \phi_r \quad (3)$$

Where, K_l is the leakage factor.

The proposed stator structure of R_{g_min} and R_{g_max} is

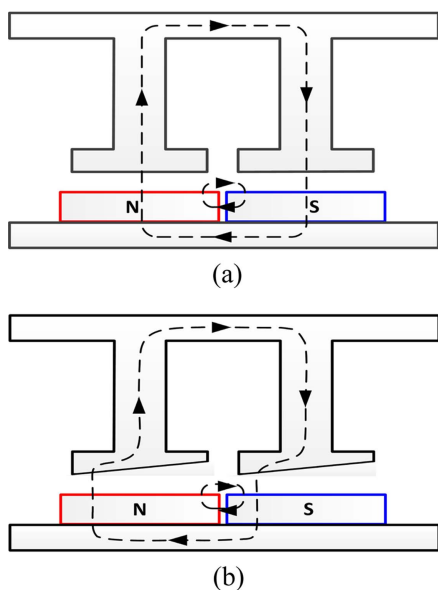


Fig. 5. (Color online) Flux Paths of (a) Initial Structure and (b) Proposed Structure.

Table 2. Design Parameter.

Design parameter	Range [mm]
Air-gap A	0.1~0.4
Air-gap B	0.1~0.7

affected by the air gap length and the cross-sectional area of the air-gap [14].

Ideally, a SPM type motor can only use the magnetic torque because this type motor does not have a magnetic saliency. As applying the asymmetric air-gap structure, the proposed model can utilize reluctance torque in addition to magnetic torque. Thus, this paper selects the direction of the motor as counterclockwise (CCW).

3. Design Optimization and FE Analysis

Asymmetric air-gap structure is designed by 2 conditions of air-gap length. As shown in Fig. 6, the maximum length of air-gap A is limited to 0.4 [mm] due to the direction of reluctance torque generation. Thus, the range of air-gap B is from 0.1 [mm] to 0.7 [mm].

Air-gap reluctance is calculated as (4)

$$\mathfrak{R} = \frac{g}{\mu A} \quad (4)$$

Where, g is air-gap length, μ is permeability and A is effective area.

As mentioned above, air-gap reluctance is linearly proportional to air-gap length so the ratio of air-gap reluctance is expressed by that of air-gap length.

The condition of air-gap and reluctance ratio which positively affects total output torque is given in (5):

$$\Delta_g = \frac{g_B}{g_A} = \frac{\mathfrak{R}_B}{\mathfrak{R}_A} > 1 \quad (5)$$

Where, g_A and g_B are minimum and maximum air-gap, Δ_g is the ratio of the air-gap and reluctance. Accordingly, the range of parameters is selected as Table 2.

Through FEA, the result values are obtained as shown in Table 3. Figure 7 shows the output power in each case as contour plot. Inasmuch the target of output power is

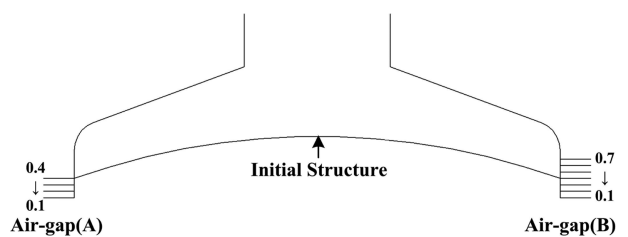


Fig. 6. Asymmetric Air-Gap Structure Design Method.

Table 3. FE Analysis Result of DOE.

Case	Air-gap A [mm]	Air-gap B [mm]	Output Power [W]	Efficiency [%]
1	0.1	0.1	0.50	63.9
2	0.1	0.2	0.67	61.8
3	0.1	0.3	0.79	61.3
4	0.1	0.4	0.89	61.3
5	0.1	0.5	0.99	60.6
6	0.1	0.6	1.09	60.1
7	0.1	0.7	1.17	59.6
8	0.2	0.1	0.63	62.9
9	0.2	0.2	0.49	63.9
10	0.2	0.3	0.82	60.2
11	0.2	0.4	0.92	63.4
12	0.2	0.5	0.92	63.2
13	0.2	0.6	1.11	58.9
14	0.2	0.7	1.19	61.8
15	0.3	0.1	0.72	61.5
16	0.3	0.2	0.79	61.6
17	0.3	0.3	0.87	59.3
18	0.3	0.4	0.97	61.5
19	0.3	0.5	1.05	57.8
20	0.3	0.6	1.14	60.6
21	0.3	0.7	1.22	60.1
22	0.4	0.1	0.79	52.8
23	0.4	0.2	0.86	60.0
24	0.4	0.3	0.93	60.1
25	0.4	0.4	1.01	57.5
26	0.4	0.5	1.09	58.8
27	0.4	0.6	1.18	59.3
28	0.4	0.7	1.26	58.9

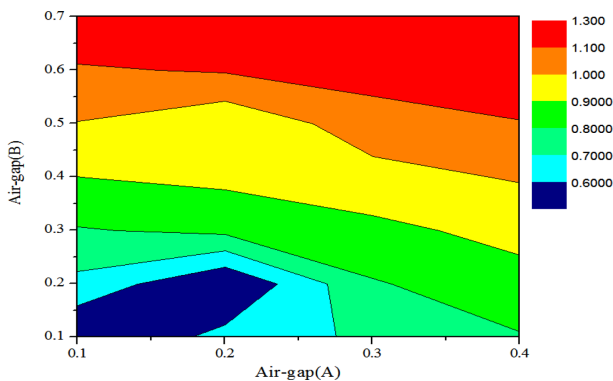


Fig. 7. (Color online) Contour Plot of Output Power.

1[W], the value under the target is excluded. The optimal air-gap design is obtained as air-gap A 0.2 [mm] and air-gap B 0.7 [mm]. The output power of the proposed model is 1.19 [W] and the efficiency of that is 61.2 [%]. The optimal model is shown in Fig. 8.

Table 4 shows the comparison of results with initial and

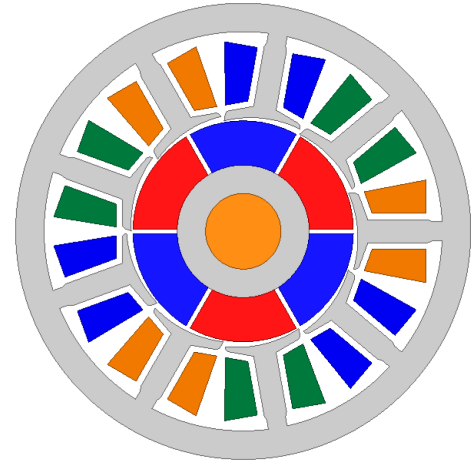


Fig. 8. (Color online) Optimal FEM Model.

Table 4. Comparison of Initial and Proposed Model.

Parameter	Initial Model	Proposed Model
Air-gap A [mm]	0.4	0.2
Air-gap B [mm]	0.4	0.7
Air-gap Ratio (Δ_g)	1	3.75
Average Air-gap [mm]	0.4	0.46
Rated Speed [rpm]	1580	1580
Input Current [A]	0.095	0.104
Output Torque [mNm]	6.1	7.23
Output Power [W]	1.01	1.19
OTPA [mNm/A]	64.01	69.63
Efficiency [%]	57.5	61.2

proposed model. OTPA of proposed model is larger than that of initial model. As mentioned above, the initial model which is SPM type BLDC motor has only alignment torque. However, as applying asymmetric air-gap structure, the proposed model can have also additional reluctance torque. Furthermore, efficiency's improvement is also obtained by about 3.7 [%].

Figure 9 shows the flux density distribution of the initial and proposed model. The difference of between maximum air-gap and minimum air-gap generates the stain on flux of stator toward the direction of motors.

4. Experimental Test

The prototype model and comparison of stator shape are shown in Fig. 10(a). The experimental test set is consisted of Dynamo set, data logger, DC supply and Speed measuring device in Fig. 10(b). Figures 11 and 12 are shown BEMF and input current through the experimental test. The efficiency comparison according to rotation speed is represented in Fig. 13. Compared with FEM results, the efficiency of the experimental test is

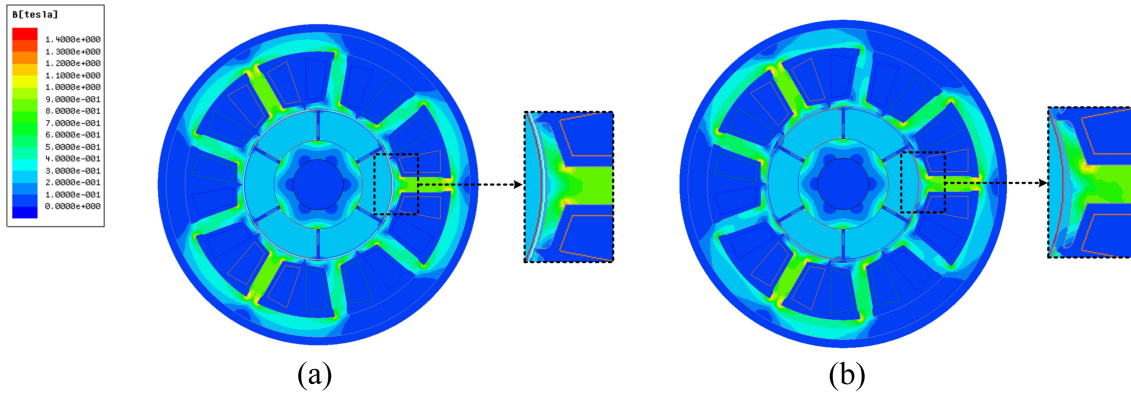


Fig. 9. (Color online) Flux Density Distribution (a) Initial Model (b) Proposed Model.

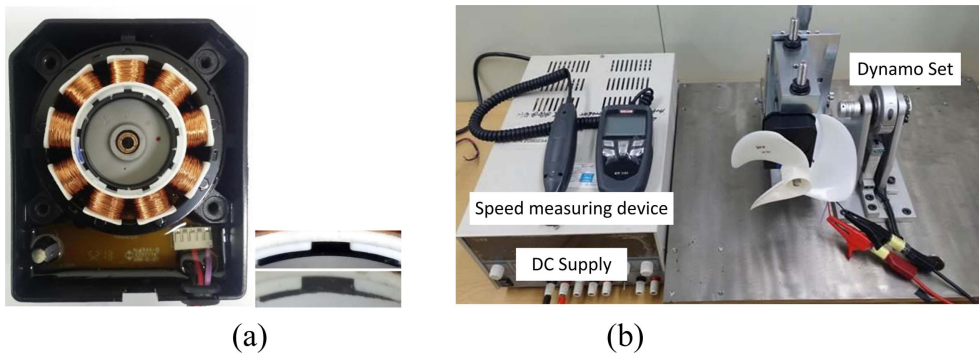


Fig. 10. (Color online) Experimental Test (a) Prototype BLDC Motor, (b) Experimental Configuration.

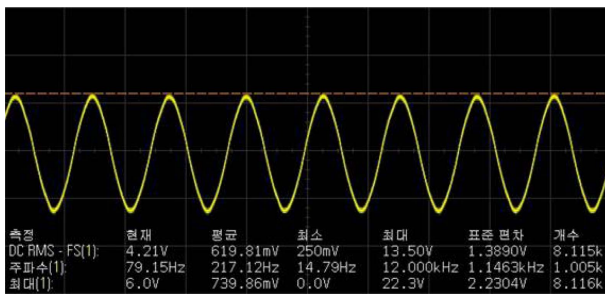


Fig. 11. (Color online) Experimental Result of BEMF.

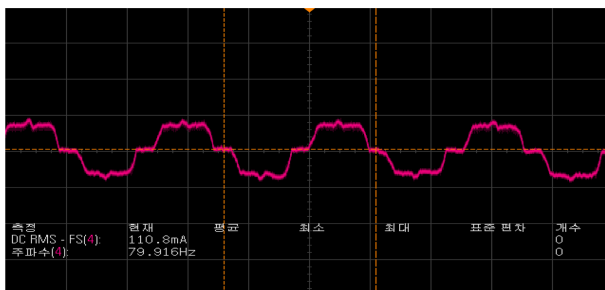


Fig. 12. (Color online) Experimental Result of Current.

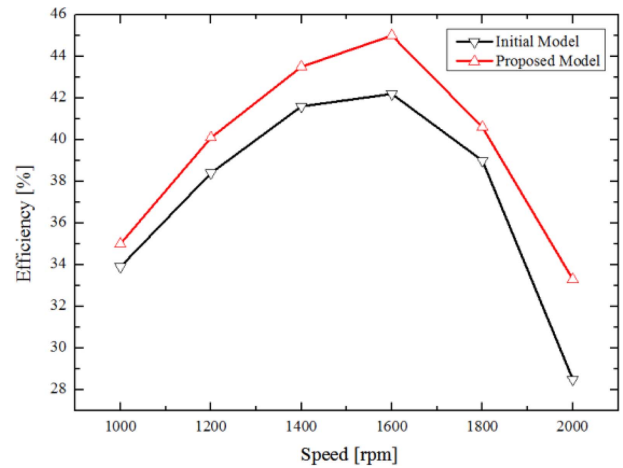


Fig. 13. (Color online) Efficiency Comparison.

efficiency is about 42.2 [%]. However, the proposed model's efficiency is increased about 2.8 [%] to 45 [%].

5. Conclusion

This paper proposed asymmetric air-gap structure in 3-phase BLDC motor for improving output characteristic and efficiency. Basically, SPM type motor has only

little lower due to losses in motor drive.

On the standpoint of efficiency, the initial model's

alignment torque. However, asymmetric air-gap structure is applied to this type motor for obtaining additional reluctance torque. The aim of the proposed structure was to obtain higher output torque by using additional reluctance torque which is produced by an asymmetric air-gap without any volume changes. Considering the rotation of the motor, the variation of air-gap is developed in counter-clockwise direction. Through optimizing the structure on FEA, the prototype has been built and experimented. The efficiency of the proposed model has been improved. Through experimental test, the validity of the proposed structure is tested. The application of asymmetric air-gap structure is an effective way to achieve high efficiency and better output characteristics.

Acknowledgment

This research was financially supported by the Ministry of Education (MOE) and National Research Foundation of Korea (NRF) through the Human Resource Training Project for Regional Innovation (NRF-2013H1B8A2028789).

References

- [1] G. Y. Sizov, D. M. Lionel, and N. O. A. Demerdash, IEEE ECCE Con. (2011).
- [2] T. Okada, Mitsubishi Electr. AD **120** (2007).
- [3] A. Consolli, G. Scelba, and M. Cacciotti, IEEE Trans. Ind. Electron. **60**, 9 (2013).
- [4] F. Lin, J. Huang, and Y. Hung, IEEE Trans. Power Electron. **25**, 10 (2010).
- [5] J. Estima and A. J. Marques, IEEE Trans. Ind. Electron. **60**, 8 (2013).
- [6] G. Foo, X. Zhang, and G. M. Vilamuthgumwa, IEEE Trans. Ind. Electron. **60**, 8 (2013).
- [7] F. Parasiliti and F. Rinaldi, IEEE Trans. Ind. Electron. **59**, 6, (2012).
- [8] M. Pacas, IEEE Magazine Ind. Electron. **5**, 2 (2011).
- [9] K. Xu, B. Panda, and L. Lam, IEEE Trans. Ind. Electron. **51**, 3 (2004).
- [10] K. Gulez, A. Adam, and H. Pastazi, IEEE Trans. Ind. Electron. **55**, 1 (2008).
- [11] J. Shao, IEEE Trans. Ind. Applic. **42**, 5 (2006).
- [12] K. H. Park, T. S. Kim, S. C. Ahn, and D. S. Hyun, IEEE Conf. **4**, 1677 (2003).
- [13] R. Saxena, Y. Pahariya, and A. Tiwary, IEEE ICCSN, IEEE, Singapore (2010) pp 583-587.
- [14] D. Hanselman, Brushless Permanent Magnet Motor Design 2nd, Magna Physics Pub., Lebanon (2006).
- [1] G. Y. Sizov, D. M. Lionel, and N. O. A. Demerdash,